

## Engine Combustion Network: “Spray A” basic measurements and advanced diagnostics

M. Meijer<sup>\*1</sup>, L-M. Malbec<sup>2</sup>, G. Bruneaux<sup>2</sup>, L.M.T. Somers<sup>1</sup>  
Eindhoven University of Technology Netherlands<sup>1</sup>, IFPEN France<sup>2</sup>  
[m.meijer@tue.nl](mailto:m.meijer@tue.nl), [louis-marie.malbec@ifpen.fr](mailto:louis-marie.malbec@ifpen.fr)

### Abstract

Diesel spray experimentation at controlled high-temperature and high-pressure conditions is intended to provide a more fundamental understanding of diesel combustion than can be achieved in engine experiments. The Engine Combustion Network (<http://www.sandia.gov/ecn>) has recently become a leading group in performing comparative studies under standardized conditions by using constant-volume pre-combustion vessels and constant flow test rigs. The purpose of this collaborative effort is to generate a high-quality dataset to be used for advanced computational model development under relevant modern diesel engine conditions.

In this study the pre-burn combustion vessel at IFPEN is used to analyze "spray A" conditions (n-dodecane, 900 K, 22.8 kg/m<sup>3</sup>, 15% oxygen). The fuel spray is characterized by applying several advanced optical diagnostic techniques. However before any spray related measurements are executed, boundary conditions inside the vessel are analyzed in great detail. The ambient gas temperature distribution before the fuel injection is measured using fast response thermocouples. The fuel temperature inside the injector is measured and then stabilized by implementing several hardware upgrades. Particle Image Velocimetry (PIV) measurements are taken in order to define ambient gas velocities inside the vessel right before fuel injection.

The spray penetration length over time is analyzed using high-speed Schlieren diagnostics. An optimized back-light illumination set-up is implemented as a replacement of the previously used Mie scattering technique. PIV measurements for reacting and non-reacting sprays are carried out to analyze the fuel spray velocities during an injection event. High-speed imaging of light luminosity and the implementation of various optical filters provides information to define the ignition delay time, ignition location and Flame Lift Off (FLO) locations.

---

### Introduction

Diesel (surrogate) fuel spray experimentation under controlled elevated temperature and pressure conditions will assist in providing a more fundamental understanding of diesel spray combustion. This level of understanding is needed to develop accurate multi-scale Computational Fluid Dynamics (CFD) models that will be used to optimize future engine designs. Surrogate fuel spray data needed for detailed model development and validation requires extensive characterization of all boundary conditions used as model inputs.

The Engine Combustion Network (ECN) group is working on performing experiments under the same injector and ambient conditions: “Spray A”, leveraging the expertise and diagnostics of each participant while enabling a direct comparison between the various facilities. The aim of the ECN work is to generate a high level combined database at engine relevant conditions. It is anticipated that the dataset developed will become a focal point for model validation and further advanced diagnostics.

“Spray A” represents a relatively low-temperature diesel engine combustion condition relevant to engines that use a moderate rate of Exhaust Gas Recirculation (EGR). The selected injector and injection pressure are based on modern common-rail injection systems. In addition to the prescribed common rail and fuel line dimensions and the location of the fuel line pressure sensor are also specified to ensure consistent hydraulic effects during injection. A single-component diesel surrogate fuel n-dodecane, is chosen to enable a complete specification of the chemical and physical properties of the fuel. Detailed chemical kinetic mechanisms exist for n-dodecane, allowing full treatment of the combustion chemistry modelling.

### Experimental set-up

Within this work, the IFPEN pre-burn type high temperature, high pressure combustion vessel is used to generate “Spray A” conditions. The ambient pressure, temperature and species at the time of injection are varied by igniting a premixed combustible-gas mixture that burns to completion. Following the spark-ignited, premixed combustion, the combustion products cool over a relatively long time, {1000-2500} ms, due to heat transfer to the vessel walls and as a result the vessel pressure slowly decreases. When the desired pressure and temperature is reached, the diesel fuel injector is triggered and fuel injection occurs. The vessel has full optical access for line-of-sight and/or orthogonal diagnostics. The vessel is cube-shaped, measuring app. 100 mm on each side, allowing extensive visualization of the spray before wall impingement. The vessels walls are (electrically) heated

---

\* Corresponding author: [m.meijer@tue.nl](mailto:m.meijer@tue.nl)

up to 200 °C, to mimic engine surface temperatures and to prevent condensation of combustion products onto the windows. Four spark plugs at the bottom of the vessel are utilized to provide consistent ignition of the fuel pre-burn lean mixture. A mixing fan stirs the gases during intake filling and afterwards in order to prevent mixture and temperature non-uniformities. Since a preburn-method is used to create high-temperature, high-pressure conditions, the composition of the initial fill reactants determines the combustion product mixture that exists at the time of fuel injection. Product mixtures may be made inert (0% O<sub>2</sub>), or to simulate EGR conditions (15% O<sub>2</sub>), for “Spray A”. More comprehensive details about the IFPEN vessel can be found in ref 1 and 2.

For ECN “spray A” experiments, the set-up is equipped with the prescribed standardized hardware such as; the fuel line, common rail, and injector. Fuel temperature is controlled using a thermostatic bath from which the set temperature is defined based on dummy injector thermocouple measurements (see also the next section: boundary conditions). The injector tip is protected by a ceramic cover to minimize the temperature increase of the injector nozzle tip as a result of the pre-burn method. Different dedicated “spray A” injectors are available within the ECN project. For the presented measurements, the “spray A” injector with serial-number 201678 and a nozzle exit diameter of 88.6  $\mu\text{m}$  is used [Ref 1]. The injector is operated by using the prescribed “spray A” injector electric current profile. Fuel line pressure is measured with a frequency of 1250 kHz at the dedicated location in the fuel line, 24 cm from the nozzle [Ref 1, 2]. Detailed SEM scans are made and analysed to study this particular injector. The main goal was to verify whether previous measurements have influenced the nozzle and injector needle surfaces (through aging effects). Based on the presented SEM scan result images from figure 1, it can be concluded that the injector did not suffer in the previous test as the surfaces are neither visually contaminated nor worn.

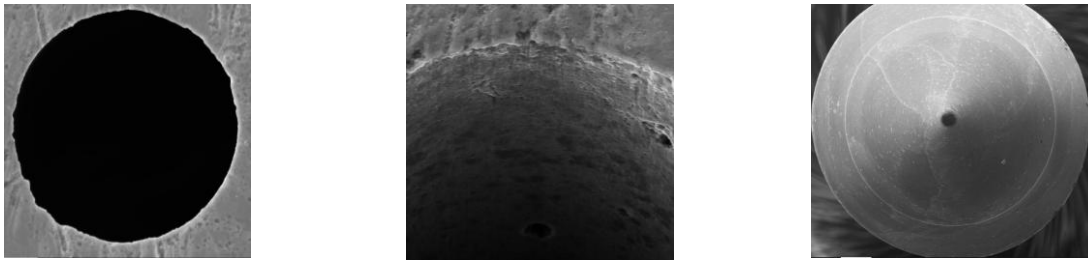


**Figure 1** SEM scans of “Spray A” injector 210678. From left to right; top and side view nozzle exit and needle.

### “Spray A” Boundary conditions

This section discusses the executed “spray A” boundary condition related measurements. Knowing and accurately controlling the experimental set-up up boundary conditions is considered to be critical in the ECN framework. Establishing and improving experimental boundary conditions in unique facilities throughout the world represents a major step forward in the establishment of high-quality, quantitative datasets for engine spray combustion.

### Ambient gas temperature distribution

Ambient gas temperature distribution characterization is or will be done by all ECN participating institutions. Fine wire type R thermocouples are recommended for pre-burn type vessels, because of the appropriate temperature range. First tests at IFPEN caused an undesirable catalytic reaction inside the set-up because of the presence of hydrogen and oxygen gasses used for the spark ignited pre-burn [ref 2]. For this measurement series, several tests were performed to avoid this (exothermic) catalytic effect which results in spontaneous ignition of the pre-burn gasses. Various tests have been executed to avoid this undesirable behaviour such as: (1) changing the filling procedure by using a N<sub>2</sub>/O<sub>2</sub> gas mixture (no filling of pure oxygen only) and (2) changing the ratio of C<sub>2</sub>H<sub>4</sub> and H<sub>2</sub> fuel. However neither had the desired effect. The result was either no ignition after spark plug activation or undesired ignition caused by the catalytic reaction with the probe. The final option was to implement Type K thermocouples (TCs). Special made prototype TCs were used with the same wire diameter of 50  $\mu\text{m}$  as the type-R TCs. Although these thermocouples are used up to their maximum temperature range, it turned out that the lifetime and measurement repeatability was satisfactory. A direct measurement approach for these TCs is implemented, which means that no signal conditioning or amplification before the DAQ system is used. Thermocouple linearization, cold junction and corrections for convection and radiation [ref 3 till 7] were implemented afterwards. Simultaneous recordings with these single TCs, at different locations inside the vessel, are taken by using 2 different mounting sides of the experimental set-up.

Averaged measurement results for various vertical positions as a function of the time after the pre-burn spark ignition are shown in figure 2. The presented temperature traces are based on five individual measurements for each position. In figure 2, results are shown where the thermocouples have been moved into the vertical (z) direc-

tion of the set-up. Similar measurements were performed by moving the thermocouple into the axial (x) direction of the fuel spray. Basic understanding of the temperature distribution as a function of time can be obtained from figures 2 and 3. After the spark ignition, the temperature in the bottom of the vessel increases first because the flame front develops from the bottom to the top (because spark plugs are located in the bottom diagonals). During the cool-down period, the cooling effect of the vessel walls becomes evident. The top of the vessel shows the highest temperature, which can be explained by buoyancy driven forces. The coolest location is found near the injector tip (right side figure 3) because of the cooling system implemented to control the fuel temperature. It can be concluded that the temperature deviation along the spray axis is {860; 910} K, with 900 K in the centre of the vessel. The bulk temperature, defined based on the bulk pressure and gas properties is 873 K. This results in a  $T_{core}/T_{bulk}$  ratio of 1.03, which is in line with earlier reported results [ref 1,2].

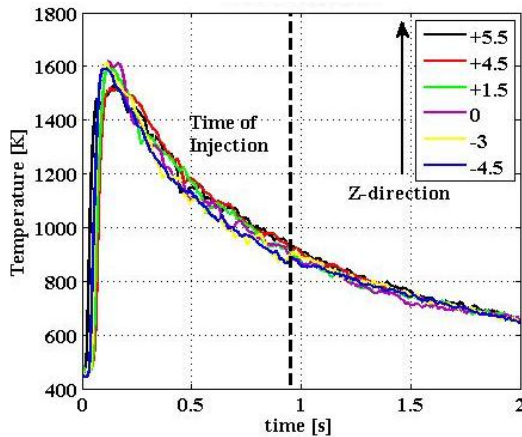


**Figure 2** Temperature traces at various vertical positions at “spray A” conditions.

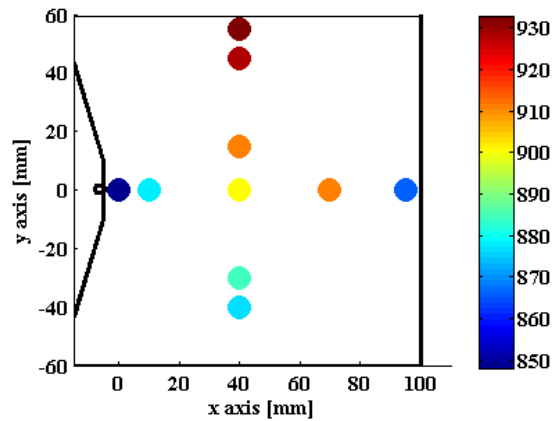


**Figure 3** Temperature fields inside the combustion vessel under “spray A” conditions. Dots indicate the position of the thermocouple inside the vessel.

### Ambient gas velocity field

“Spray A” bulk gas velocity is prescribed to be  $\leq 1$  m/s [ref 1] but no verifications regarding this boundary condition have yet been published for pre-burn type vessels. Applying Particle Induced Velocity (PIV) diagnostics is a convenient method to analyse these velocity fields. A schematic overview of the PIV set-up used is shown in figure 4. Seeding of the ceramic spherical particles with a diameter of  $\leq 5$   $\mu\text{m}$ , is done by adding them into the nitrogen gas (which is one of the gasses to fill before pre-burn), by using a dedicated particle seeding device [ref 8]. A double pulsed high speed laser of 512nm is used at 10 kHz with a pulse delay of 10  $\mu\text{s}$  and pulse energy of 10 MJ. A high-power pulsed laser sheet is created to make the particles visible in the ambient. Images are captured with a high speed camera (Photron SA1).

Post-processing of the obtained raw images is done by using a commercially available software package: Insight 3G. An interesting question is how the use of the internal fan throughout the complete experiment (from pre-burn until the end of fuel spray injection) will influence the velocities of the gas. Both cases are measured: having the fan deactivated 1s before spark ignition or leaving the fan on throughout the complete measurement. Gas velocities are near-quiescent when the fan is turned off just before the pre-burn event. Maximum speeds of 1 m/s are measured. With the fan activated the distribution of velocities within the vessel increases slightly, at a maximum of approx. 5 m/s. The result of these 2 cases are presented in figure 5, showing the gas velocity distribution immediately before Start Of Injection (SOI). Although this measured speed is negligible compared to the velocities measured within a Diesel spray, the fan will be turned off for PIV measurements.

### Fuel temperature

Among the limit conditions that need to be controlled, one is the temperature of the injected fuel. This temperature will have a significant impact on the mixing and combustion processes [ref 9, 10]. Moreover, the injected fuel temperature is one of the main input variables for CFD models. Therefore, the injected fuel temperature has to be accurately measured and controlled. For this purpose, Sandia designed a so-called “dummy” injector, equipped with a high-speed time-resolved K-type thermocouple. The extremity of this thermocouple is placed in the sac volume of the injector, and its distance to the nozzle tip can be adjusted. This dummy injector is equal to the other “spray A” injectors except that the needle is pierced to allow for the TC, and there is no nozzle hole. [ref 2 and 11].

A non-institutive ceramic shield was added around the nozzle tip body in order to limit the thermal flux from hot ambient gases towards the injector. The effectiveness of this cover has been addressed earlier in [ref 11]. Figure 6 shows the measured temperatures inside the injector nozzle at various locations (0mm represents the nozzle tip) with and without the use of a ceramic cover. Comparison with data from the TU/e reveals the same tempera-

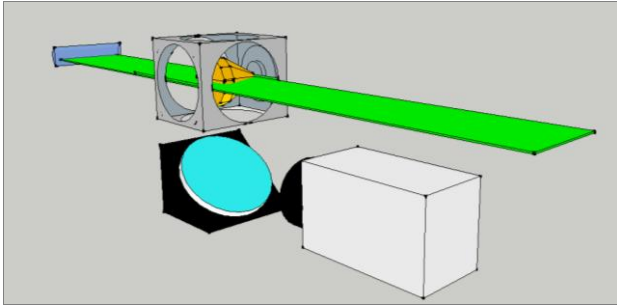


Figure 4 Schematic overview of the PIV set up.

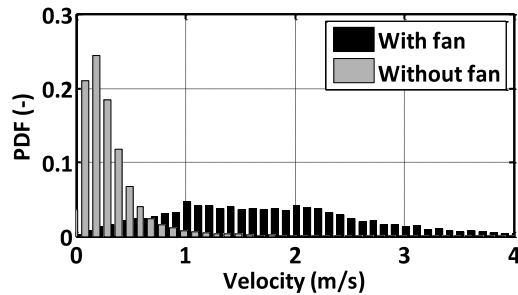


Figure 5 PDF of the velocities norms in the field of view. With (black) and without (gray) activated fan.

ture increase directly after the pre-burn event [ref 11]. It can be observed that the fuel temperature increase, especially close to the injector tip, is significant when the ceramic cover is absent. A maximum increase of approximately 30 K is measured without any protection at 0 mm. Using a ceramic cover will reduce the local fuel temperature uncertainty to only +/- 5 K at SOI. The impact on important spray variables, such as the liquid length, will be addressed in the next section.

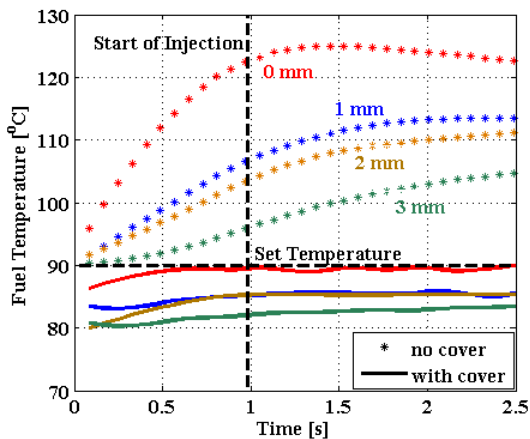


Figure 6 Local fuel temperatures inside the injector tip.

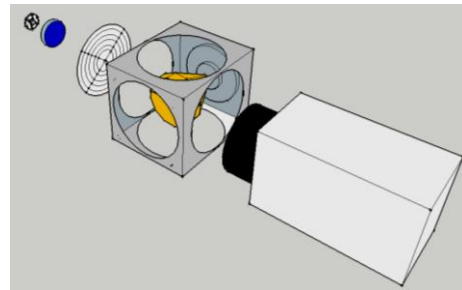


Figure 7 Schematics DBI set-up

### Liquid length based on diffuser back-light illumination

The Liquid Length (LL) is generally defined as the maximum distance from the injector tip to liquid-phase fuel penetration for an evaporating fuel spray [ref 12,13]. The liquid length is a fundamental parameter for spray model validation. Recent studies have shown that slight differences in the experimental technique, as well as the calibration and post-processing, could lead to large variations in the measured liquid length [ref 14]. Being aware of the problems related to the measurement of liquid-phase penetration in evaporative sprays, the participants of the ECN agreed to use Diffused Back-Illumination imaging (DBI) to standardize results. The described measurement set-up and post-processing algorithms described in this section are all related to this standardized ECN "spray A" methodology [ref 13]. One reason for selecting DBI is that the incident illumination without the spray provides an intensity reference that can be used to determine the global extinction when light is attenuated by the spray. For DBI, rays are collected from multiple angles along various paths. Although beam-steering still occurs for any single ray, the integration of multiple rays onto a single pixel has the effect of smoothing the effects of beam steering on the two-dimensional results.



The light used to illuminate the spray comes from a LED light source ( $460 \pm 10$  nm) in combination with a diffuser and a Fresnel lens. The diffuser is a  $50^\circ$  square pattern and the field lens in this case is a simple Fresnel lens with a focal length of 152 mm. Rather than collimation of the incoming light, a diffused bundle of rays is directed towards the spray. Images are captured by using a Photron SA1 high speed camera with a frame rate of 120 kHz. A 50 mm camera lens is used in combination with a 8 mm extension ring. Figure 7 shows the optical setup used for diffused back-illumination imaging.

The DBI method is based on the measurement of the light extinction through the liquid core. The reference level is the background of the image when there is no liquid injection. A mean image of the background,  $\langle I_{BG} \rangle$  is thus necessary. Next each image during the injection can be divided by the background image, in order to obtain the normalized intensity of the image. The logarithm of the normalized intensity gives the extinction factor  $\tau$  in the whole visualization field:

$$\tau(x, y) = -\log\left(\frac{I(x, y)}{\langle I_{BG} \rangle(x, y)}\right) \quad (3)$$

Finally, the evolution of  $\tau$  along the spray axis is considered to measure the liquid length. To measure the steady-state liquid length,  $\tau$  is computed on a time-averaged image, during the steady-state period of the injection. About 10 injections are performed to obtain an ensemble average together with shot-to-shot standard deviation. As explained above, this technique suffers from beam steering near the liquid spray tip, due to the refractive index gradient created by the vaporized fuel. Therefore the exact liquid length is not measured precisely, but the decay of the extinction factor along the spray axis can be fitted by a slope that intercepts 0, giving a value for the liquid length (figure 11). Measurement results are shown in table 1 for different ambient gas temperatures and injector configurations (with or without the ceramic cover). An interesting observation is that the standard deviation seems to decrease (absolutely and relatively to the average LL length) when the ambient gas temperature increases. Also the impact of the ceramic cover becomes clear, resulting in a 1.65 mm shorter LL when not used.

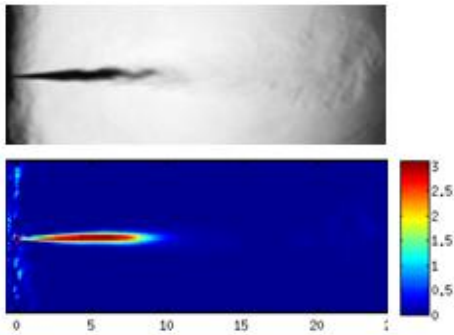


**Figure 8** Liquid Length penetration results for spray A conditions. Single shot image (top) & averaged steady LL region images showing the normalized intensity.

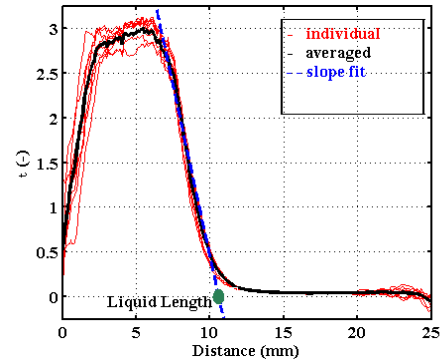


**Figure 9** Post-processing result of LL measurements at Spray A conditions.

	800K	900K	1000K
678 with cover	11.6 +/-0.3mm	10.2 +/-0.3mm	8.1 +/- 0.2mm
678 no cover	n.m.	8.6 +/-0.2mm	n.m.

**Table 1** Liquid length results for different gas temperatures at “spray A” conditions.(n.m.: not measured)

### Spray penetration

Vapour penetration of the spray was measured by using Schlieren diagnostics. The experimental set-up consists of a continuous wave LED light source (455 nm at 1.1 W) which is focused using an objective, passing through a pinhole to simulate an infinite small light source. A dichroic mirror is used to make a parallel light beam. This beam is focused again by using a positive lens. Images are captured with a high speed camera at 30 kHz. The spatial filter is a 5 mm disc that blocks the non-deviated rays. As a result, the vapour will appear in bright on a dark background. Ten injection events were performed in order to obtain an average penetration and its associated standard deviation. The post-processing algorithm used is the ECN standard, developed by Sandia. As the spray appears as a bright region on the images, an algorithm based on intensity manages to detect its edges. The penetration distance is defined according to Naber and Siebers [15], where a 50% probability criterion for penetration within the inner half-angle of the spray is used. The measurement of the vapour penetration gives an indi-

cation of the core density within the vessel. The results are presented in figure 11. It appears that with a core density of 22.8 kg/m<sup>3</sup>, the vapour penetration measured at IFPEN is slightly lower than that reported by Sandia (Figure 11), although the difference between them is smaller than the standard deviation down to 1.4ms. However a change in the core density from 22.8kg/m<sup>3</sup> to 21.8kg/m<sup>3</sup> gives a better correlation between Sandia’s and IFPEN’s results, as can be seen on Figure 11

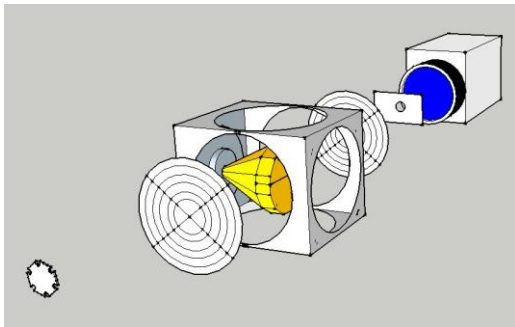


Figure 10 Schematic Schlieren set-up

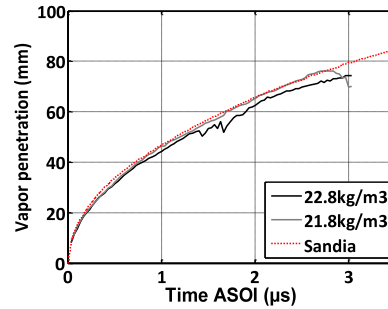


Figure 11 Spray penetration results for different densities around spray A conditions

**Flame Lift Off Length**

The lift-off length of the flame was measured through the direct detection of the light emission of the OH\* radical at 310nm, with an intensified camera and a bandpass filter (313 +/- 7.5 nm). The signal is integrated over 500µs during the steady-state period of the flame: 1100-1600µs after the electric command of injector. This gives the mean value of the lift-off length. The post-processing of the lift-off length images consists of defining reference intensity and then taking 50% of this reference intensity as a threshold value for the lift-off length determination [ref 16, 17]. An example of the images obtained is presented in Figure 12. The measured lift-off length is in agreement with Spray A conditions, but has been obtained with a T<sub>core</sub>/T<sub>bulk</sub> ratio of 1.05, which is slightly higher than the 1.03 resulting from temperature measurements. With a T<sub>core</sub>/T<sub>bulk</sub> ratio of 1.03, the measured lift-off length was about 15.5mm. In order to be consistent with the ECN standards, in the following measurements a T<sub>core</sub>/T<sub>bulk</sub> ratio of 1.05 has been used.

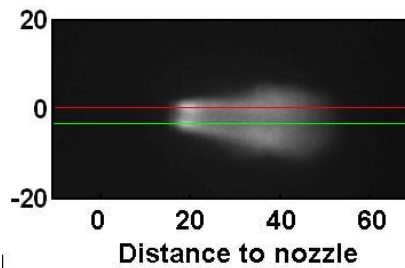


Figure 12 Time average OH\* image at “Spray A”.

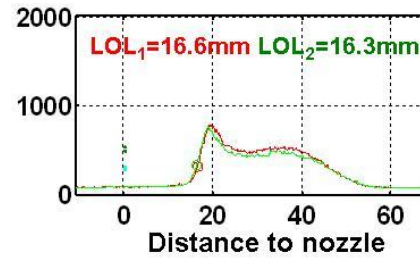


Figure 13 Intensity profiles along the spray axis.

**Ignition delay**

The goal of the ignition delay measurements is to capture the first emission of light from the start of ignition. Images of the combustion were acquired without filter, at a frame rate of 30 kHz and a long exposure time (93 µs), to maximize the sensitivity of the light detection. With such a setup, the detection of the cool flame is possible, together with the onset of high-temperature combustion (Figure 14). However the camera chip is saturated when soot incandescence appears. The results of ignition delay are in line with the lift-off length measurement, even if, in these results, the ignition delay is less sensible than lift-off length to the modification of the T<sub>core</sub>/T<sub>bulk</sub> ratio. An ignition delay of about 400µs is obtained, similar to spray A standards.

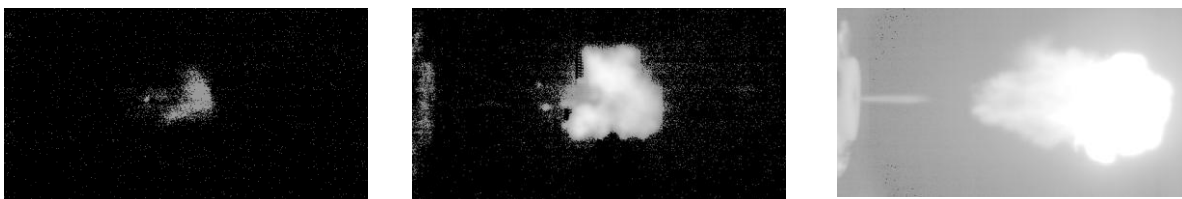
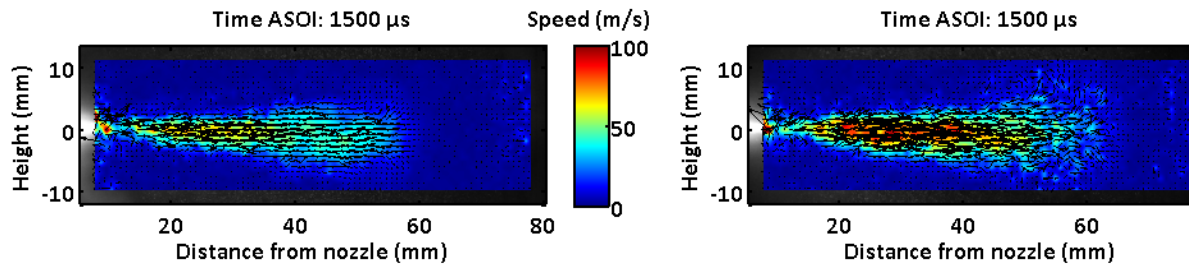


Figure 14 Image sequence of the start of ignition; moving from left to right; showing the evolution from cool flame to ignition. t=0.30 ms: cool flame; t=0.45ms: high-temperature ignition; t=0.90 ms: soot incandescence.

### Velocity field

After defining the boundary conditions necessary to achieve “spray A” conditions, measurements of the velocity fields within the jet were performed. These measurements have been achieved through time-resolved PIV at 20 kHz (a velocity field every 100 $\mu$ s). The images were acquired by a Photron SA1 camera equipped with a Nikkor lens, 50mm f/1.4. The laser sheet was produced by a high-speed YAG laser at 532nm, and intercepted the spray on its axis. The layout of the setup and the seeding are similar to the earlier presented set-up shown in figure 6. The velocity fields are averaged over 20 injection events. Two examples are displayed in figure 17 for reacting and non-reacting cases.



**Figure 17** Ensemble averaged images of PIV fields in non-reacting (left) and reacting (right) conditions.

The evolution of the velocities within the spray is analysed in detail. The axial velocities at various timings and the transverse velocities at various distances from the nozzle tip have been extracted from the velocity fields. The results are presented on figures 18 and 19. For clarity reasons, the standard deviations are not displayed, but they were estimated to be of the order of +/- 5m/s.

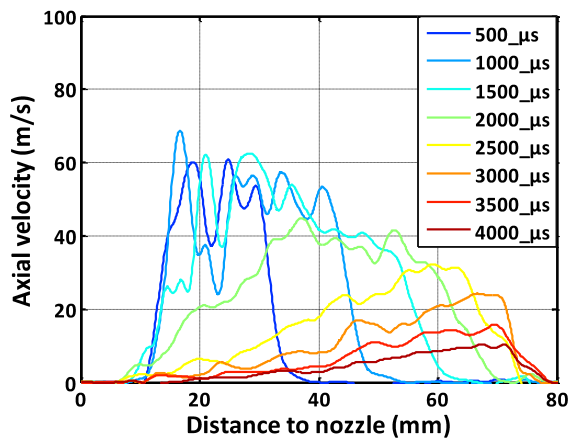


**Figure 18** Axial velocities at different timings after the Start Of Injection (SOI), non-reacting condition.

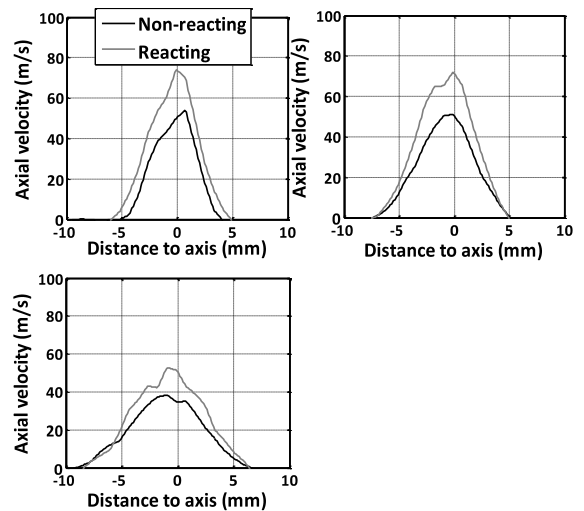


**Figure 19** Transverse velocities profiles at different distances (25mm top-left, 35mm top-right, 45mm bottom-left) from the nozzle tip. Velocities profiles are time-averaged during the steady state.

Near the orifice exit (i.e. below 20mm), the spray velocities are not accessible because of several reasons: first the proximity of the liquid core generates a high intensity Mie scattering signal that interferes with the particle imaging, also the density of particles is low in this region because not enough particles have yet been entrained in the spray (only the ambient is seeded), as a result the PIV post processing is very probably not accurate in this region, finally the time delay between the two PIV images (4 $\mu$ s) might also not be appropriated for the high velocities existing in this region of the jet. Therefore only velocity measurement downstream 20mm are to be considered. It is to note that this is also downstream of the lift-off length. Figure 18 shows the formation of a steady state velocity profile before the End Of Injection (EOI), which occurs at 1500 $\mu$ s. Indeed, the axial velocities are converging to the same value of about 50-60 m/s. The same behaviour can be observed in the reacting case, although the maximum velocities are more important, around 70-80m/s. The transverse velocities profiles displayed in figure 19 show the same difference between reacting and non-reacting cases. The spray is accelerated in the reacting case. This result is consistent with the higher vapour penetration obtained in reacting conditions compared to non reacting [ref 2] and is very probably due to gas expansion effects associated with the heat released by the diffusion flame. After EOI, the velocities in the spray decrease very rapidly (Figure 18), in particular in the tail region. This result is consistent with previous work [8] and is due to the air entrainment dynamic after EOI.

## Summary and Conclusions

The boundary conditions were measured in great detail inside the pre-burn vessel at IFPEN in order to match the “spray A” conditions. The temperature of the fuel is set to 90°C, through the measurements of the temperature in the sac volume of a dummy injector. The temperature distribution within the vessel was also measured, showing a good homogeneity as long as the gases are not too close to the walls. Moreover, a relation between the bulk and the core density has been defined. Based on these measurements, the boundary conditions are characterized.

After defining and controlling these boundary conditions, basic diagnostics were performed to access the characteristics of the mixing and combustion processes of the n-dodecane fuel spray. Liquid length measurements showed good agreement with earlier reported “spray A” standards, together with the vapour penetration, even if concerning this latter, a slight deviation was observed. Based on combustion diagnostics, it appeared that the temperature at the SOI was slightly higher than 900K. This was corrected by an adaptation of the bulk density. After this correction, the measurements of the velocity fields within the spray were performed, giving access to velocity profiles that can be used for model validation. Also significant differences were observed between reacting and non-reacting cases, due to the gases expansion associated with heat release, and generating an acceleration of the velocities within the jet. However, the following further work is necessary:

- Through the characterization of boundary conditions, a certain degree of uncertainty on the exact core density was observed when analysing the vapour penetration results. Measurements of velocity fields at different bulk densities can help assessing the impact of this uncertainty on the resulting velocity fields
- Variations in the fuel injection pressure and the core density could be helpful for model validation and will be performed.

## References

- [1] Official ECN website: <<http://www.sandia.gov/ecn/>>
- [2] Pickett, L., M., Genzale, C., Bruneaux, G., Malbec, L.-M., Hermant, L., Christiansen, C., Schramm, J., Comparison of diesel spray combustion in different high-temperature, high pressure, facilities, SAE international, SAE2010-01-2106, 2010.
- [3] L Michalski, K. Eckersdorf, J Kucharski, J. McGhee, Temperature Measurements *Second Edition*, 2001 John Wiley & Sons Ltd.
- [4] W. M. Pitts, E. Brown, R. D. Peacock, H. E. Mitler, Temperature uncertainties for Bare-Bead and aspirated thermocouple Measure in fire environments, ASTM international 2002.
- [5] Miles, P.C., Gouldin, F.C., "Determination of the time constant of fine-wire thermocouples for compensated temperature measurements in premixed turbulent flames" Comb. Sci. Tech. 83:1-19, 1992.
- [6] Petit, C., Gajan, P., Lecordier, J.C., and Paranthoen, P., "Frequency response of fine-wire thermocouple", J. Phys. E: Sci. Instrum., 15:760, 1982.
- [7] Dupont, A., Paranthoen, P., Lecordier, J.C. and Gajan, P., "Influence of temperature on the frequency response of fine-wire thermocouples over the range (300 K-800 K) in airflows", J. Phys. E: Sci. Instrum., 17:808-812, 1984.
- [8] Bruneaux, G., Maligne, D., Study of the Mixing and Combustion Processes of Consecutive Short Double Diesel Injections, *SAE Int. J. Engines* 2(1):1151-1169, 2009.
- [9] Payri, R., Garcia-Oliver, J.M., Bardi, M, Manin, J., Fuel temperature influence on diesel sprays in inert and reacting conditions, *Applied Thermal Engineering* 35 (2012), 185-195
- [10] Payri, R., Garcia-Oliver, J.M., Bardi, M, Manin, J., Fuel temperature influence in Diesel spray in reactive conditions, ICLASS2011-163, 2011
- [11] M.Meijer, R.J. Christians, J.G.H. v. Griensven, L.M.T. Somers, L.P.H. de Goey. Engine Combustion Network: implementation and analysis of combustion vessel spray A conditions, ICLASS-Americas NA 23rd conference 2011, paper 151.
- [12] Siebers, D.L., Scaling liquid-phase fuel penetration in Diesel sprays based on mixing-limited vaporization SAE-1999-01-0528, 1999.
- [13] J. Manin, M. Bardi and L.M. Pickett. Evaluation of the liquid length via diffused back-illumination imaging in vaporizing diesel sprays. The eighth international conference for modeling and diagnostics for advanced engine systems (COMODIA 2012), 2012.
- [14] L.M Pickett, C.L. Genzale, J. Manin, L.-M. Malbec, and L. Hermant. Measurement uncertainty of liquid penetration in evaporating diesel sprays. ICLASS-Americas 2011, Ventura, CA, 2011.
- [15] Naber, J.D., Siebers, D.L., Effects of Gas Density and Vaporization on Penetration and Dispersion of Diesel Sprays, SAE Paper 960034, 1996
- [16] Higgins B., Siebers D.L. "Diesel-spray ignition and premixed burn behavior." SAE Paper 2000-01-0940.
- [17] Pickett, L.M., Siebers, D.L., Idicheria, C.A, Relationship Between Ignition Processes and the Lift-Off length of Diesel Fuel Jets, SAE paper 2005-01-3843, 2005.